Chinese Chemical Letters 34 (2023) 107201

Contents lists available at ScienceDirect

Chinese Chemical Letters

journal homepage: www.elsevier.com/locate/cclet

Thiophene-based covalent organic frameworks for highly efficient iodine capture

Xi Yan[a], Yixin Yang[a], Guorong Li[a], Jianhua Zhang[c], Yu He[a], Ran Wang[a], Zian Lin[a,*], Zongwei Cai[b]

[a] Ministry of Education Key Laboratory of Analytical Science for Food Safety and Biology, Fujian Provincial Key Laboratory of Analysis and Detection Technology for Food Safety, College of Chemistry, Fuzhou University, Fuzhou 350108, China
[b] State Key Laboratory of Environmental and Biological Analysis, Department of Chemistry, Hong Kong Baptist University, Hong Kong, China
[c] Radiation Environment Supervision Station of Fujian Province, Fuzhou 350001, China

ARTICLE INFO

Article history:
Received 14 November 2021
Revised 19 December 2021
Accepted 3 February 2022
Available online 6 February 2022

Keywords:
Thiophene-based covalent organic frameworks
Iodine
Morphology
Adsorption mechanisms
Radioactive seawater

ABSTRACT

Development of adsorbent materials for highly efficient iodine capture is high demand from the perspective of ecological environment and human health. Herein, the two kinds of thiophene-based covalent organic frameworks (COFs) with different morphologies were synthesized by solvothermal reaction using thieno[3,2-*b*]thiophene-2,5-dicarbaldehyde (TT) as the aldehyde monomer and tri(4-aminophenyl)benzene (PB) or tris(4-aminophenyl)amine (PA) as the amino monomer (denoted as PB-TT COF and PA-TT COF) and the as-prepared two heteroatoms-rich COFs possessed many excellent properties, including high thermal stability and abundant binding sites. Among them, PB-TT COF exhibited ultra-high iodine uptake up to 5.97 g/g in vapor, surpassing most of adsorbents previously reported, which was ascribed to its high specific surface (1305.3 m^2/g). Interestingly, PA-TT COF with low specific surface (48.6 m^2/g) showed good adsorption ability for iodine in cyclohexane solution with uptake value of 750 mg/g, which was 2.38 times higher than that obtained with PB-TT COF due to its unique sheet-like morphology. Besides, the two COFs possessed good reusability, high selectivity and iodine retention ability. Based on experimental results, the adsorption mechanisms of both COFs were studied, revealing that iodine was captured by the physical-chemical adsorption. Furthermore, the both COFs showed excellent adsorption ability in real radioactive seawater treated safely, demonstrating their great potential in real environment.

From the perspective of energy supply and environmental protection, nuclear energy plays the extremely vital role in many countries and regions [1]. However, environmental issues related to nuclear energy are attracting more and more public attention. As one of the volatile products in nuclear waste, radioiodine easily diffuses into the air to make it difficult to handle in the actual environment [2,3]. In addition, radioactive pollution caused by iodine (I_2) would last for over ten million years because of extremely long half-life of iodine [4]. It is well-known that radioactive iodine released from Fukushima and Chernobyl nuclear power incidents directly influence human metabolism by bioaccumulation in the food chain, thereby increase the incidence of diseases such as thyroid cancer [5,6]. Therefore, the effective treatment of radioactive iodine is essential to the long-term development and application of nuclear energy.

At present, porous adsorbent materials, including porous carbon [7,8], porous organic polymers (POPs) [9,10], metal-organic frameworks (MOFs) [11,12] have been developed to adsorb iodine because of their high surface area, porosity and uniform pore properties [13]. However, porous carbons usually show poor efficiency for iodine adsorption due to lack of sufficient active sites. Amorphous POPs do not provide highly ordered internal structures and full accessibility to active sites in the frameworks [14]. MOFs often cannot tolerate high temperature and high humidity, which hamper its adsorption ability in practical application [15]. As a result, the design and development of novel porous adsorbent materials with abundant binding sites and excellent physical/chemical stability are of great significance for iodine capture.

Covalent organic frameworks (COFs), as a class of porous crystalline material with periodic structure connected by organic building units *via* covalent bonds, have attracted great attention due to its unique properties such as high surface area, high porosity, excellent thermal stability, ordered channel structure, low density as well as structural diversity [16,17].

* Corresponding author.
E-mail address: zianlin@fzu.edu.cn (Z. Lin).

https://doi.org/10.1016/j.cclet.2022.02.007
1001-8417/

The fascinating features of COFs show great application in gas adsorption, sensing, energy conversation and catalysis [18–23]. Especially, COFs are also regarded as excellent adsorbents for iodine capture. For instance, Jiang *et al.* reported TPB-DMTP COF (TPB = triphenylbenzene; DMTP = dimethoxyterephthaldehyde) and TTA-TTB COF (TTA = 4,4′,4″-(1,3,5-triazine-2,4,6-triyl)trianiline; TTB = 4,4′,4″-(1,3,5-triazine-2,4,6-triyl)tribenzaldehyde)), which can effectively capture iodine due to their large surface areas [24]. However, most studies of COFs-based iodine capture are still limited to exploitation of large surface areas and high porosity of porous adsorbents [25,26]. Besides, previous studies showed that the incorporation of affinity sites (such as enriched π-electron, nitrogen or sulfur-rich heteroatom groups) into the polymeric skeletons would contribute to capture iodine [27]. Despite some progress for iodine capture has been achieved, it is rarely reported that COFs with unique morphology and affinity sites obtained by precise design were used to capture iodine.

Inspired by the above-mentioned studies, two kinds of thiophene-based COFs with different morphologies, rich heteroatoms, extended π-conjugations and abundant pore structure were synthesized by thieno[3,2-*b*]thiophene-2,5-dicarbaldehyde (TT) and tri(4-aminophenyl)benzene (PB) or tris(4-aminophenyl)amine (PA) as building blocks though Schiff-base condensation reaction. The as-obtained PB-TT COF and PA-TT COF could serve as an excellent adsorbent for iodine capture in vapor and solution. In addition, their adsorption mechanisms were studied by series of experimental investigation. The practicability of both COFs to capture iodine from real environment sample was also discussed in this work.

The synthetic route of the COFs was presented in Fig. 1a. The preparation of both COFs was completed by one-pot condensation reaction using TT as the aldehyde monomer and PB or PA as the amino monomer, respectively. In order to further verify the successful synthesis of COFs, the corresponding characterizations were conducted. The FT-IR spectra of both COFs were represented in Figs. S1a and b (Supporting information). Characteristic peak of −C=N of PB-TT COF appeared at 1663 cm^{-1}, along with the disappearance of the −N−H (3434 and 3353 cm^{-1}) stretching vibrations of PB and the −C=O (1648 cm^{-1}) vibration of TT. The peak of −C=N of PA-TT COF appeared at 1656 cm^{-1}, along with the disappearance of vibration band of −C=O (1648 cm^{-1}) and the −N−H (3405 and 3336 cm^{-1}) of PA, indicating the successful Schiff-base condensation reaction. The crystallinity of both COFs was studied by powder X-ray diffraction (PXRD) and the result was displayed in Figs. S1c and d (Supporting information). The power diffraction peaks of PB-TT COF were well in accordance with the literature previously reported [28]. Compared with the crystallinity of PB-TT COF, PA-TT COF showed relatively fewer characteristic peaks and obviously broad peak. The poor crystallinity of PA-TT COF might be ascribed to weakened rigidity of backbone owning to easy twist of PA monomer [29]. The thermal stability of both COFs was analyzed by thermogravimetric analysis (TGA) (Figs. S2a and b in Supporting information), and the weight loss of the PB-TT COF with temperature as high as 450 °C was about 3%. For PA-TT COF, it showed a slight weight loss up to 200 °C because of the loss of the trapped solvent and H_2O [30]. When temperature was increased to 450 °C, the residue of the PA-TT COF was over 87 wt%. The results mentioned above indicated high thermal stability of both COFs.

The porous structure and specific Brunauer-Emmett-Teller (BET) surface area of both COFs were measured by N_2 sorption isotherms at 77 K. According to the nitrogen adsorption isotherms (Figs. 1b and c), the BET surface areas of PB-TT COF and PA-TT COF were 1305.3 m^2/g and 48.6 m^2/g, respectively. Compared with PB-TT COF, PA-TT COF showed much lower specific surface areas, which

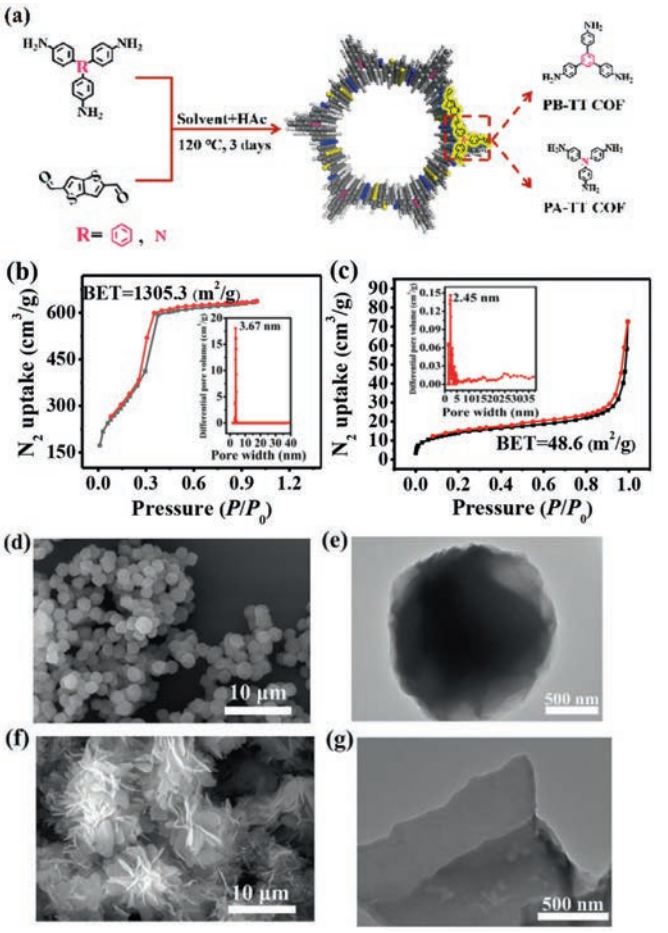

Fig. 1. (a) Synthetic scheme of COFs. (b) N_2 adsorption-desorption isotherms of PB-TT COF (inset: the pore size distribution of PB-TT COF). (c) N_2 adsorption-desorption isotherms of PA-TT COF (inset: the pore size distribution of PA-TT COF). (d) SEM image of PB-TT COF. (e) TEM image of PB-TT COF. (f) SEM image of PA-TT COF. (g) TEM image of PA-TT COF.

could be attributed to its poor crystallinity. The pore sizes of PB-TT COF and PA-TT COF were 3.67 nm and 2.45 nm, respectively, which were obtained by calculating nonlocal density functional theory (NLDFT) (Figs. 1b and c). In addition, the total pore volumes of PB-TT COF were calculated to be 0.986 cm^3/g at P/P_0=0.996. For PA-TT COF, its total pore volumes were 0.112 cm^3/g at P/P_0=0.994 (Table S1 in Supporting information). The morphological structures of PB-TT COF and PA-TT COF were analyzed by SEM and TEM. It was clearly seen that PB-TT COF showed spheres-like morphology (Figs. 1d and e). Whereas, PA-TT COF exhibited sheet-like morphology (Figs. 1f and g). The EDX analysis of the corresponding PB-TT COF and PA-TT COF were showed in Figs. S2c and d (Supporting information), indicating the two kinds of COFs contained rich heteroatoms. However, PB-TT COF had more heteroatoms than that of PA-TT COF.

Considering the porous characteristics and heteroatoms (nitrogen and sulfur)-containing structures of both COFs, they are potentially efficient for capturing iodine. Therefore, gravimetric measurements were conducted to investigate adsorption performance of both COFs for vapor iodine under typical fuel reprocessing conditions (75 °C and 1 K) [31]. The mass of glass bottles containing the COFs were weighted at various time intervals in the process of adsorbing iodine. With time going by, the color of both COFs exposed to I_2 vapor gradually darkened owing to continuous capturing iodine of the COFs (Fig. 2a). The result in Fig. 2a indicated the

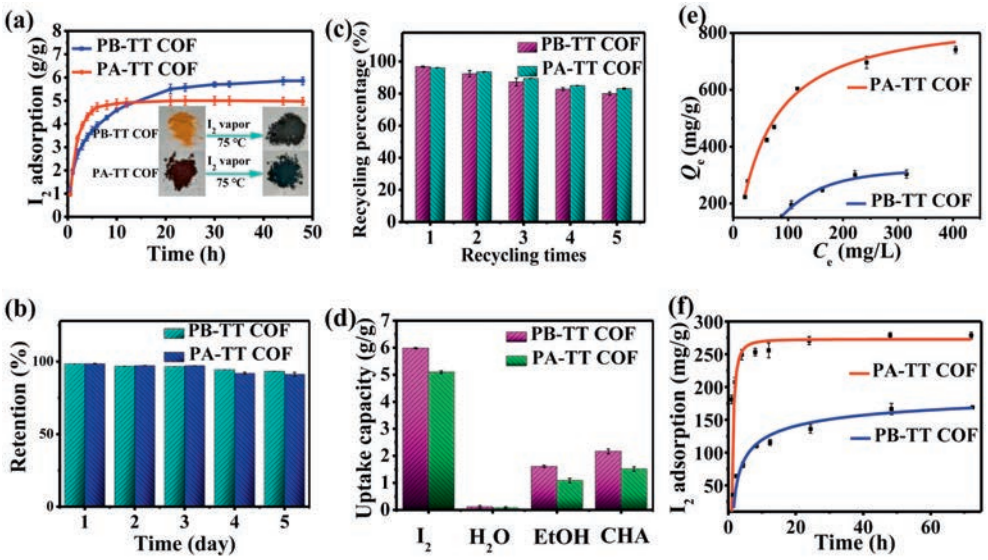

Fig. 2. (a) Gravimetric iodine adsorption of the two COFs as a function of time at 75 °C and 1 bar (inset: the photographs of the COFs before and after I_2 vapor adsorption). (b) Iodine retention of iodine-captured COFs upon exposure to air at 25 °C and 1 bar. (c) Reusability of both COFs for iodine adsorption. (d) The adsorption selectivity of both COFs for I_2, H_2O, EtOH and CHA. (e) Adsorption isotherm for iodine in cyclohexane of the two COFs. (f) Adsorption kinetic curve for iodine in cyclohexane of the two COFs.

iodine uptake capacity of COFs increased sharply during the first 10 h and then slowly increased until saturated. The equilibrium adsorption capacities were measured to be 5.97 g/g and 5.1 g/g for PB-TT COF and PA-TT COF, respectively. The adsorption ability of PB-TT COF was higher than that of PA-TT COF, which were in good agreement with the TGA analysis, clearly indicating that I_2@PB-TT COF and I_2@PA-TT COF had the weight loss of 72.5% and 67.8%, respectively. As far as we know, the I_2 uptake capacity of PB-TT COF (5.97 g/g) exceeded most of the reported adsorbents, such as silver doped adsorbents, carbon materials, MOF, POPs and other COFs (Table S2 in Supporting information). The high iodine capture ability of PB-TT COF may be ascribed to the synergistic effect of high specific surface areas and affinity binding sites (N and S) in skeleton.

In addition, COFs adsorbed iodine could maintained their weight upon exposure to air under ambient conditions (25 °C and 1 bar), which showed that iodine penetrated into the pores and did not escape from the frameworks of COFs (Fig. 2b). The phenomena indicated that COFs not only adsorb effectively, but also steadily store iodine in their pores. Reusability of adsorbents is extremely important factor in practical applications. COFs adsorbed iodine could be regenerated by heating at 120 °C under vacuum. Then, regenerated materials were used for next adsorption experiment under the same condition. The two COFs can still maintain good adsorption ability after 5 cycles (Fig. 2c). Selective experiments were carried out with iodine, water, ethanol and cyclohexane (CHA) at 75 °C and ambient pressure, which indicated that the adsorption capacities of both COFs toward iodine was higher than water, ethanol, and cyclohexane (Fig. 2d). Especially, the two COFs hardly adsorb water, which was extremely important for practical applications due to containing abundant moisture in nuclear fuel reprocessing.

Encouraged by their outstanding performance of adsorbing iodine vapor, the I_2 adsorption ability of both COFs in cyclohexane solution was assessed quantitatively using UV–visible spectra by monitoring absorption intensity (Fig. S3 in Supporting information). The purple solution faded gradually over time by adding the COFs to solution (Fig. S4 in Supporting information), which indicted iodine of cyclohexane solution captured by the COFs. I_2 adsorbing capacity of COFs is a key index to evaluate performance of adsorbents. As presented in Fig. 2e, the ability of adsorbing iodine of PA-TT COF was 2.38 times higher than that of the PB-TT COF. The maximum adsorption ability of both COFs were 750 mg/g and 315 mg/g, respectively, surpassing a lot of adsorption materials previously reported (Table S3 in Supporting information). Equilibrium adsorption isotherms of both COFs were both well-fitted with the Langmuir model (Fig. S5 in Supporting information). As shown in Fig. 2f, according to adsorption kinetic curve for iodine in cyclohexane (250 mg/L) of both COFs, adsorption equilibrium of PA-TT COF and PB-TT COF was reached at 12 h and 72 h, respectively. The adsorption kinetic process of both COFs was fitted with the pseudo-second-order kinetic model (Fig. S6 in Supporting information), which indicated that chemisorption-type processes occurred and there was a strong interaction between the adsorbent and iodine molecules [32]. The adsorption performance in solution of PA-TT COF was superior to PB-TT COF no matter adsorption capacity or adsorption rates, which may be mainly ascribed to unique sheet-like morphology and more N atoms in the skeleton. The sheet-like PA-TT COF may serve as a shelter, where iodine can be stored in the narrow slit between the papery sheets. For PB-TT COF, though it showed higher specific surface areas, it was more difficult to store iodine due to its solid structures and agglomerated spheres, which contribute to lower iodine capturing capacity in cyclohexane, which were clearly demonstrated by previous studies [33,34].

The iodine capture mechanism of both COFs was studied by a combination of FT-IR, XPS and Raman analysis. Firstly, I_2@PB-TT COF and I_2@PA-TT COF were analyzed through FT-IR spectroscopy. Compared with FT-IR spectra of pristine COFs, the stretching vibration peak of the –C=N of I_2@PB-TT COF and I_2@PA-TT COF showed significant shift from 1663 cm^{-1} to 1650 cm^{-1} for PB-TT COF and from 1656 cm^{-1} to 1627 cm^{-1} for PA-TT COF, respectively (Figs. 3a and b). These FT-IR changes showed that had charge-transfer interaction between iodine and N atom of the imine linkage of COFs, indicating existence of chemisorption process. Moreover, the species of iodine captured in COFs were investigated by the XPS spectra (Fig. S7 in Supporting information). As seen from Figs. 3c and d, it was observed that the two obvious peaks were located at 618.0 and 629.5 eV for I_2@PB-TT COF, and 619.35 and 629.75 eV for I_2@PA-TT COF, which were attributed to I $3d_{5/2}$ and I $3d_{3/2}$ orbitals of I_2 molecules, respectively. Besides, another two peaks at 620.3, 631.7 eV for I_2@PB-TT COF and 621.3, 630.85 eV for I_2@PA-TT

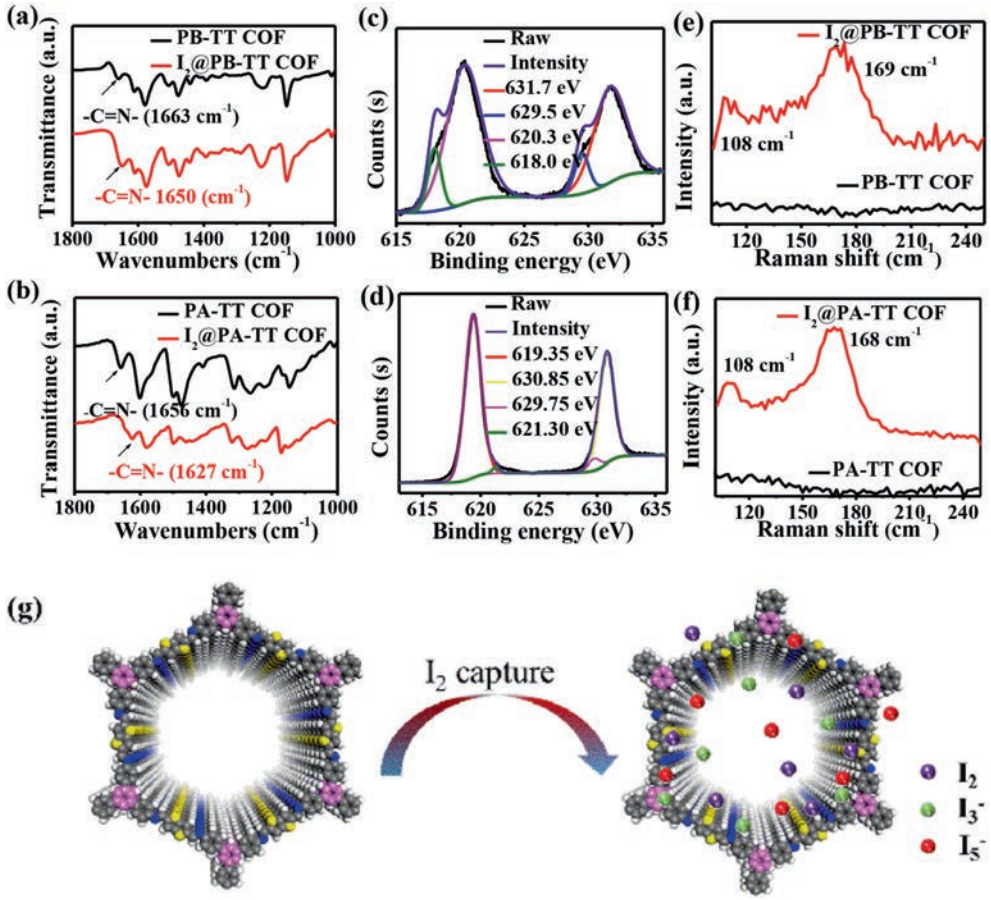

Fig. 3. (a) FT-IR spectra of PB-TT COF and I_2@PB-TT COF. (b) FT-IR spectra of PA-TT COF and I_2@PA-TT COF. (c) XPS spectra of iodine for I_2@PB-TT COF. (d) XPS spectra of iodine for I_2@PA-TT COF. (e) Raman spectra of PB-TT COF and I_2@PB-TT COF. (f) Raman spectra of PA-TT COF and I_2@PA-TT COF. (g) Iodine uptake mechanism of COFs.

COF were observed, respectively, which indicated the existence of polyiodine anions (such as I_3^- and I_5^-) in the pore. Besides, the peak intensity and binding energy of S affinity sites produced by thiophene have obviously changed after iodine capture (Fig. S8 in Supporting information). Furthermore, the adsorbed iodine species were further investigated by Raman spectroscopy and the results were displayed in Figs. 3e and f. Unlike pure COFs that showed no distinct peaks, I_2@PB-TT COF and I_2@PA-TT COF showed distinct peaks at 108, 169 cm^{-1} and 108, 168 cm^{-1}, respectively. The peaks at both 108 cm^{-1} and 169, 168 cm^{-1} can be assigned to the symmetric stretching vibration of I_3^- and stretching vibration of polyiodide I_5^-, respectively. According to the obtained results, it could be deduced that absorbed iodine species in two COFs existed as I_2 molecules and polyiodine anions. Based on above results, mechanism of iodine vapor capture could be inferred (Fig. 3g). Firstly, the iodine vapor was adsorbed into the pores via physisorption, then formed the charge complexes with N atoms in the skeleton of COFs, indicating that the existed chemisorption. Obviously, the physisorption and chemisorption contributed to the ultrahigh iodine capture. The adsorption mechanism was similar with previous work [32].

To further assess iodine adsorption ability of both COFs in real environment, adsorption experiments of both COFs were executed in radioactive seawater treated safely from local Nuclear Emergency Command Center. However, there was no iodine detected in radioactive seawater obtained by UV-visible spectra. The corresponding experiments with spiked with iodine in the real environment samples were conducted to further evaluate iodine adsorption ability of the two heteroatoms-rich COFs. As shown in Fig. 4a,

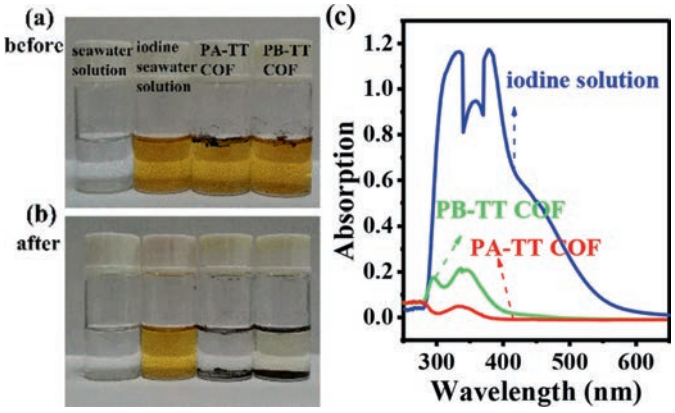

Fig. 4. (a) The photograph of seawater solution before iodine adsorption. (b) The photograph of seawater solution after iodine adsorption. (c) UV-visible absorption spectra of iodine solution before and after adsorption.

the color of seawater spiked with iodine showed yellow, both COFs were floating on the surface of solution because of their low density. The glass bottles having solution were shaken at 250 rpm in thermostatic orbit incubator. It was clearly seen from Figs. 4a and b that the color of solution with PA-TT COF had obvious change from yellow to colorless, yellow solution with PB-TT COF finally became light yellow. The UV-visible spectra (Fig. 4c) further showed that the absorption peaks of iodine in seawater were decreased significantly, indicting excellent iodine adsorption ability of both COFs

and adsorption ability of PA-TT COF was higher PB-TT COF. The results were consisted with the aforementioned experimental results of iodine adsorption in cyclohexane solution. Overall, the adsorption performance of PA-TT COF was superior to PB-TT COF in solution, no matter in cyclohexane solution or seawater solution. The above results also indicated that both COFs had promising potential in real environment.

In summary, two heteroatoms-rich COFs with different morphologies were synthesized by one-pot Schiff-base condensation reaction of TT with PB or PA. The obtained COFs showed excellent performances involving high thermal stability and abundant binding sites, in addition to the high specific surface and unique morphology. Taking these advantages together, the two COFs exhibited excellent iodine adsorption ability in vapor and solution. The iodine capture ability of PB-TT COF with high specific surface in vapor phase was 5.97 g/g, surpassing most of adsorbents previously reported. PA-TT COF with sheet-like morphology showed ultrahigh iodine adsorption performance in cyclohexane solution with an uptake of up to 750 mg/g. Moreover, the adsorption mechanism was studied by related experiments, revealing that iodine was captured by a combined process of physisorption and chemisorption. In addition, the two COFs exhibited excellent adsorption ability in radioactive seawater treated safely, indicating that both COFs adsorbents are potential in real environment.

Declaration of competing interest

The authors declare that they have no known competing financial interests or relationships that could have appeared to influence the work reported in this paper.

Acknowledgments

This work was supported by the Major Scientific and Technological Innovation Project of Shandong (No. 2021CXGC010705), and National Natural Science Foundation of China (Nos. 91843301, 22036001 and 21974021).

Supplementary materials

Supplementary material associated with this article can be found, in the online version, at doi:10.1016/j.cclet.2022.02.007.

References

[1] X. Zhang, I.D. Silva, H.G.W. Godfrey, et al., J. Am. Chem. Soc. 139 (2017) 16289–16296.
[2] M. Janeta, W. Bury, S. Szafert, Appl. Mater. Interfaces 10 (2018) 19964–19973.
[3] B.J. Riley, J.D. Vienna, D.M. Strachan, et al., J. Nucl. Mater. 470 (2016) 307–326.
[4] W. Xie, D. Cui, S. Zhang, Y. Xu, D. Jiang, Mater. Horiz. 6 (2019) 1571–1595.
[5] Z. Yin, S. Xu, T. Zhan, et al., Chem. Commun. 53 (2017) 7266–7269.
[6] S. Xu, S.P. Freeman, X. Hou, et al., Environ. Sci. Technol. 47 (2013) 10851–10859.
[7] J. Zhou, S. Hao, L. Gao, et al., Ann. Nucl. Energy 72 (2014) 237–241.
[8] H. Sun, P. La, R. Yang, et al., J. Hazard. Mater. 321 (2017) 210–217.
[9] X. Qian, B. Wang, Z. Zhu, et al., J. Hazard. Mater. 338 (2017) 224–232.
[10] Q. Borjihan, Z. Zhang, X. Zi, et al., J. Hazard. Mater. 384 (2020) 121305.
[11] P. Chen, X. He, M. Pang, et al., ACS Appl. Mater. Interfaces. 12 (2020) 20429–20439.
[12] C. Falaise, C. Volkringer, J. Facqueur, et al., Chem. Commun. 49 (2013) 10320–10322.
[13] Y. Zhu, Y. Qi, X. Guo, et al., J. Mater. Chem. A 9 (2021) 16961–16966.
[14] Y. Xie, T. Pan, Q. Lei, et al., Angew. Chem. Int. Ed. 60 (2021) 22432–22440.
[15] M. Xu, T. Wang, L. Zhou, et al., J. Mater. Chem. A 8 (2020) 1966–1974.
[16] L.A. Baldwin, J.W. Crowe, D.A. Pyles, et al., J. Am. Chem. Soc. 138 (2016) 15134–15137.
[17] Y. Du, H. Yang, J.M. Whiteley, et al., Angew. Chem. Int. Ed. 55 (2016) 1737–1741.
[18] M. Lohse, T. Bein, Adv. Funct. Mater. 28 (2018) 1705553.
[19] X. Wang, X. Han, J. Zhang, et al., J. Am. Chem. Soc. 138 (2016) 12332–12335.
[20] H. Xu, J. Gao, D. Jiang, Nat. Chem. 7 (2015) 905–912.
[21] M. Wu, Y. Yang, Chin. Chem. Lett. 28 (2017) 1135–1143.
[22] Z. Huang, Q. Xua, X. Xu, Chin. Chem. Lett. 31 (2020) 2495–2498.
[23] X.Li Y.Yan, G. Chen, et al., Chin. Chem. Lett. 32 (2021) 107–112.
[24] P. Wang, Q. Xu, Z. Li, et al., Adv. Mater. 30 (2018) 1801991.
[25] J. Chang, H. Li, J. Zhao, et al., Chem. Sci. 12 (2021) 8452–8457.
[26] X. Guo, Y. Li, M. Zhang, et al., Angew. Chem. Int. Ed. 59 (2020) 22697–22705.
[27] S. Xiong, J. Tao, Y. Wang, et al., Chem. Commun. 54 (2018) 8450–8453.
[28] L. Ascherl, T. Sick, J.T. Margraf, et al., Nat. Chem. 8 (2016) 310–316.
[29] R. Xia, X. Zheng, C. Li, et al., ACS Nano 15 (2021) 7638–7648.
[30] D. Chen, Y. Fu, W. Yu, et al., Chem. Eng. J. 334 (2018) 900–906.
[31] Z. Yan, Y. Yuan, Y. Tian, et al., Angew. Chem. Int. Ed. 54 (2015) 12733–12737.
[32] J. Li, H. Zhang, L. Zhang, et al., J. Mater. Chem. A 8 (2020) 9523–9527.
[33] F. Ren, Z. Zhu, X. Qian, et al., Chem. Commun. 52 (2016) 9797–9800.
[34] S. Xiong, X. Tang, C. Pan, et al., ACS Appl. Mater. Interfaces 11 (2019) 27335–27342.